Grant Agreement no. 226967
Seismic Hazard Harmonization in Europe

Project Acronym: SHARE

SP 1-Cooperation

Collaborative project: Small or medium-scale focused research project

THEME 6: Environment

Call: ENV.2008.1.3.1.1 Development of a common methodology and tools to evaluate earthquake hazard in Europe

D4.5– Vector predictions

Due date of deliverable: 01.06.2011

Actual submission date: 31.12.2012

Start date of project: 2009-06-01 Duration: 36

Middle East Technical University (METU)

M. A. Sandıkkaya, S. Akkar

Revision: 1

Dissemination Level

PU	Public	x
PP	Restricted to other programme participants (including the Commission Services)	
RE	Restricted to a group specified by the consortium (including the Commission Services)	
CO	Confidential, only for members of the consortium (including the Commission Services)	

SHARE

SEISMIC HAZARD HARMONIZATION IN EUROPE

WP4: STRONG GROUND MOTION MODELLING

GROUND-MOTION PREDICTION EQUATIONS ON VERTICAL-TO-HORIZONTAL SPECTRAL AMPLITUDE RATIOS AND DAMPING FACTORS FOR VECTOR-VALUED PROBAILISTIC SEISMIC HAZARD CALCULATIONS

M.A. Sandıkkaya and S. Akkar

Earthquake Engineering Research Center,
Middle East Technical University,
06800 Ankara, Turkey

December, 2012

Table of Contents

List of Tables

List of Figures

Introduction

Several engineering applications (base isolated buildings, bridges etc) require the response spectrum to be defined at damping levels other than 5% of critical. In addition, vertical seismic hazard becomes crucial especially for designing short-period structural systems at long return periods. The recent trend in probabilistic seismic hazard assessment (PSHA) is to develop ground-motion prediction equations (GMPEs) for 5%-damped horizontal spectral ordinates that can be modified for different damping levels as well as for vertical ground motion that are compatible with target hazard scenario (e.g., Gülerce and Abrahamson 2011; Bommer et al. 2011; Rezaeian et al., 2012). This report presents the vector-based ground-motion prediction equations for vertical-to-horizontal (V/H) spectral amplitudes and scaling factors for viscous damping levels other than 5% damping. The proposed equations are compatible with the currently proposed horizontal GMPE of Akkar et al. (2013) in terms of estimator parameters and range of applicability as they are based on the same strong-motion database; the subset of SHARE strong-motion databank. The report also includes the epsilon-based correlation coefficients for the horizontal and V/H GMPEs for the computation of conditional mean spectrum (CMS) proposed by Baker (2011). Provided the rationale behind its derivation (Baker and Cornell (2005), the CMS is currently accepted as the most appropriate spectrum and it is derived from a site-specific PSHA study for seismic design and verification of structural systems. It is believed that the products presented in this report will primarily serve for the vector-valued probabilistic seismic hazard assessment studies in the broader Europe region.

Strong-Motion Database

The database compiled for this study is a subset of the strong-motion databank that is developed for the Seismic Hazard Harmonization in Europe (SHARE) project (Yenier et al., 2010). The database consists of strong-motion accelerograms from the pan-European region and it is also used for the derivation of updated pan-European predictive model for 5%-damped horizontal spectral ordinates. The moment magnitude (M_w) range of the database is between 4 and 7.6. The database consists of recordings up to 200 km in terms of R_{JB} distance measure (closest

distance to the surface projection of fault rupture). Figure 1 shows the M_w vs. R_{JB} distribution of the database for different style-of-faulting (SoF) and V_{S30} (time based average of 30 m thickness of soil media) bins. The specific features of the database are discussed in Akkar et al. (2013) and the reader is referred to that study for further explanations and limitations of the accelerometric data used in this study.

The horizontal and vertical spectral ordinates at 14 different damping levels (i.e., 1%, 2%, 3%, 4%, 5%, 6%, 7%, 8%, 9%, 10%, 15%, 20%, 25% and 30%) are computed from the compiled strong-motion database for developing the V/H and damping GMPEs. The geometric mean values of the horizontal components are calculated for PGA, PGV and 18 periods (0.01s-4.0s) and used as horizontal ground-motion throughout this study. The critical usable period for each accelerogram is computed by using the criteria set in Akkar and Bommer (2006).

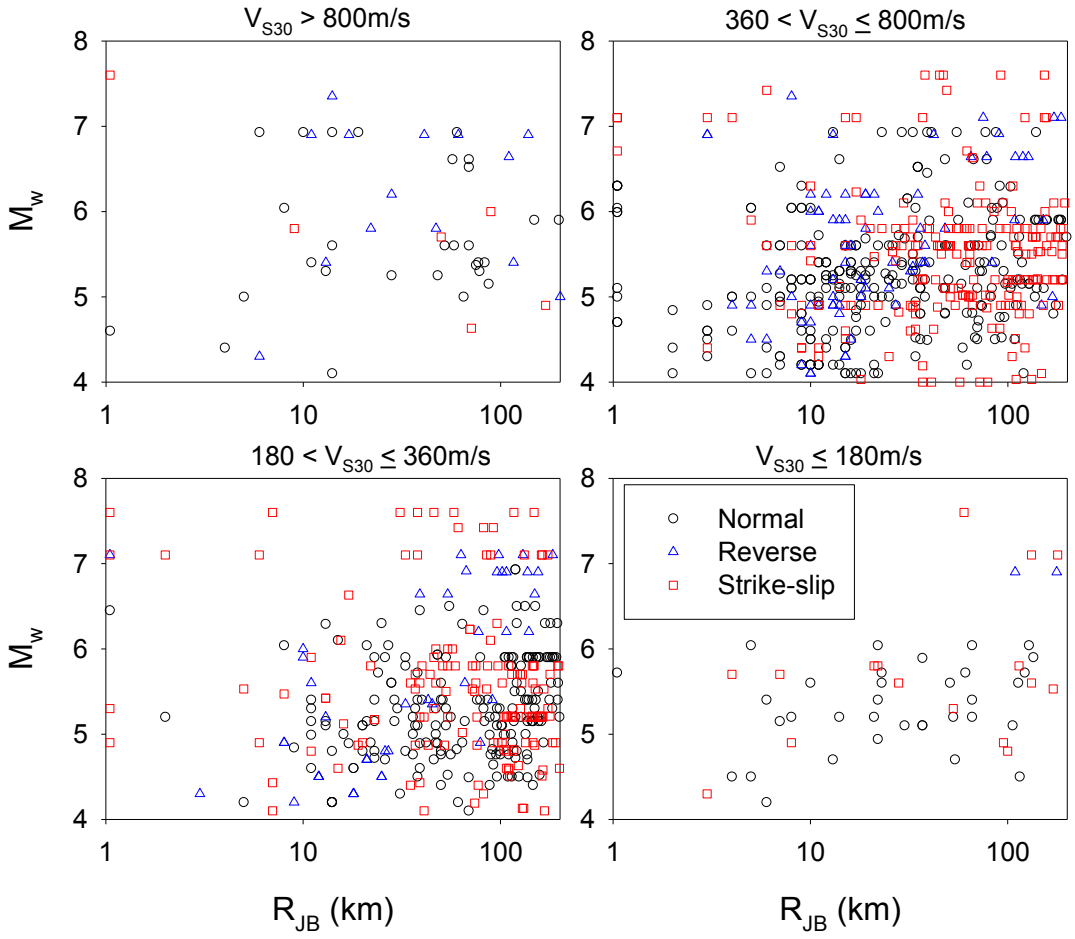

Figure 1. Distribution of the database in terms of magnitude, distance (R_{JB}), style-of-faulting and different V_{S30} bins.

Predictive equations for damping scaling factors

The model development for damping scaling factor, DSF, the ratio of pseudo-spectral acceleration (PSA) at different damping levels (β) to PSA at 5% damping (Eq. 1) as well as the possible model estimators are discussed in detail by Rezaeian et al. (2012). Previous models for DSF are generally expressed by the damping level, β and spectral vibration period, T (e.g., Malhotra, 2006). Few models discussed the effects of other parameters on DSF. For example, Abrahamson and Silva (1996) included M_w as a predictor variable in their model; Stafford et al. (2008) emphasized the significance of duration in DSF; Cameron and Green (2007) considered the effect of tectonic regime on DSF estimations; Hartzigeorgiou (2010) found that site class plays a role in DSF variation; Rezaeian et al. (2012) showed that the trend in DSF can be described sufficiently by magnitude and source-to-site distance as the estimator parameters.

$$DSF = \frac{\text{PSA at } \beta\% \text{ damping}}{\text{PSA at } 5\% \text{ damping}} \tag{1}$$

In this study the natural logarithm of DSF is regressed against M_w, R_{JB}, SoF and V_{S30} for each damping level. Other estimator parameters are not included in the DSF model (e.g., duration) as they may complicate the hazard studies that would possibly use the proposed expressions. The preliminary regression results showed that that a bilinear magnitude function or inclusion of higher order magnitude terms for magnitude scaling do not yield improvements in DSF estimations. The magnitude-dependent slope term in geometrical distance decay also did not play an efficient role on the median DSF trends. None of these complicated functions in magnitude and distance scaling decreased the standard deviation of the model as well. The preliminary regression indicated a trend in terms of style-of-faulting but its effect is overlooked in the final model as normal to strike slip and reverse to strike-slip ratios are close to unity. Thus, the style-of faulting effect is not modelled in the final equation. The averages of residual distributions for each SoF are almost zero that also validates disregarding the style-of-faulting effect in the final DSF model. It should be noted that the style of faulting distribution in the strong-motion database is poor and ignoring its effect on DSF variation may not reflect the genuine behavior of this parameter. The fictitious depth term is also kept constant for all spectral periods to have a smooth variation in spectral shape. Consideration of fictitious depth as an

independent parameter did not change the model estimations, which advocates its minimal effect in DSF predictions. The final functional form of the DSF GMPE is given in Eq. 2.

$$\ln(DSF) = c_1 + c_2 * (M_w - 5) + c_3 * \ln(\sqrt{R_{JB}{}^2 + 25}) + c_4 * \ln\left[(V_{S30} / V_{REF})\right] \quad (2)$$

In the above expression, c_i (i = 1 to 4) are period-dependent regression coefficients. The previous model developers on DSF (e.g., Trifunac and Lee, 1989; Boore et al., 1993; Bommer et al., 1998; Berge-Thierry et al., 2003; Facciolli et al., 2004; Akkar and Boomer, 2007) provide different set of regression coefficients for each damping level. This methodology is not followed in this study and the regression coefficients c_1 to c_4 are expressed as a polynomial that is a function of damping factor, β, as given in Eq. (3).

$$c_i = b_{i1} + b_{i2} \ln(\beta) + b_{i3} \ln(\beta)^2 \quad (3)$$

The primary aim of this approach is to increase the applicability of the model. Newmark and Hall (1982) are the first proponents of such polynomial functions as given in Eq. (3). In their paper, Newmark and hall (1982) proposed a first-order polynomial. The analytical studies of this report tried polynomial functions of different order. The observations from these studies indicated that a second-order polynomial is sufficient to explain the data trend. Figure 2 illustrates a sample comparison between the performances of the second- and third-order polynomials. The comparative plots indicate that the more complicated third-order polynomial does not bring a significant improvement over the simpler second-order polynomial. Bommer et al. (2000) suggested a rationale function instead of a polynomial expression as presented here that is still in use by Eurocode 8 (CEN, 2004). The rationale function was used as one of the alternatives while developing the model but this functional form was abandoned in the later stages of this study because the resultant DSF estimations were unrealistic. Table 1 presents the horizontal spectral ordinate DSF regression coefficients b_{ij} for each c_i where i varies from 1 to 4 and j varies from 1 to 3. In a similar way, Table 2 lists the vertical spectral ordinate regression coefficients

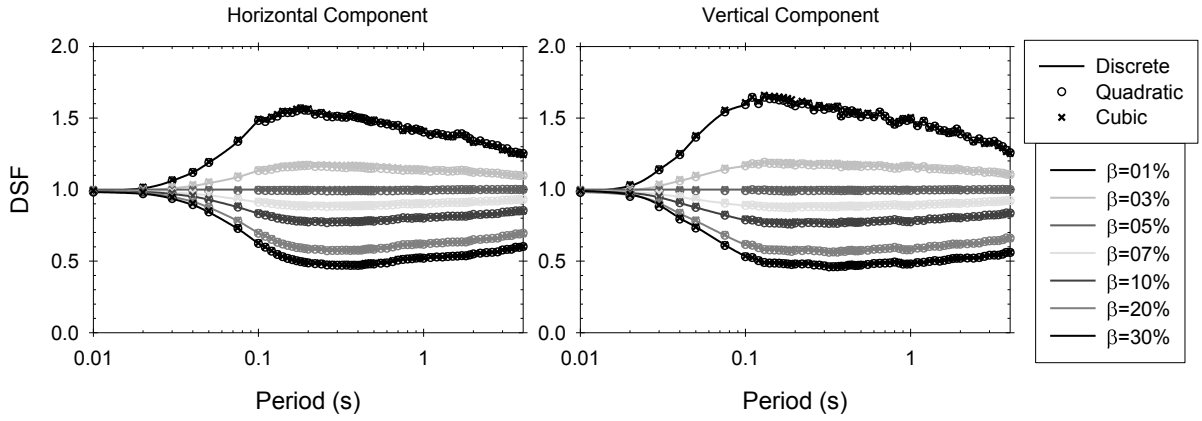

Figure 2. Comparison of discrete, quadratic and cubic regressions

Table 1. DSF regression coefficients for horizontal spectral ordinates

T(s)	b_{11}	b_{12}	b_{13}	b_{21}	b_{22}	b_{23}	b_{31}	$b_{3,2}$	$b_{3,3}$	$b_{4,1}$	$b_{4,2}$	$b_{4,3}$
0.01	-0.00023	-0.00238	-0.00136	0.000079	-0.00014	0.000398	0.000025	0.000265	-0.00012	-7.4E-05	0.001075	-0.00083
0.02	-0.00023	-0.03316	0.00041	0.000076	0.000819	-0.00048	0.000027	0.006291	-1.1E-05	-6.4E-05	-0.00157	-1.2E-05
0.03	-0.0002	-0.10813	0.009051	0.00007	0.003383	0.00065	0.00002	0.020144	-0.00189	-0.00007	-0.01173	0.000965
0.04	-0.00021	-0.18804	0.006596	0.000074	0.014343	0.001142	0.000023	0.031734	-0.00081	-6.6E-05	-0.02786	0.00176
0.05	-0.00021	-0.26703	-0.00103	0.000073	0.020318	0.00462	0.000025	0.042706	0.000778	-6.4E-05	-0.03807	0.001237
0.075	-0.00024	-0.38487	-0.02489	0.000073	0.030856	0.008131	0.000033	0.051189	0.006016	-5.9E-05	-0.04602	-0.00066
0.1	-0.00021	-0.42096	-0.05118	0.000074	0.028916	0.011298	0.000029	0.040311	0.010651	-0.00004	-0.07361	-0.00393
0.15	-0.0002	-0.42873	-0.08844	0.000054	0.023097	0.009933	0.000029	0.026715	0.015074	-0.00004	-0.05796	-0.01166
0.2	-0.00019	-0.37179	-0.08616	0.000051	0.013218	0.010404	0.000026	0.006835	0.011845	-3.4E-05	-0.0382	-0.01225
0.3	-0.00021	-0.29388	-0.07961	0.000058	0.001965	0.007841	0.000031	-0.01177	0.007578	-4.9E-05	-0.01256	-0.01298
0.4	-0.00021	-0.2285	-0.06878	0.000059	-0.00737	0.006512	0.000034	-0.02756	0.004239	-4.1E-05	-0.00348	-0.0087
0.5	-0.00026	-0.21451	-0.06277	0.000064	-0.01884	0.002234	0.00004	-0.02547	0.004178	-0.00006	0.014104	-0.0007
0.75	-0.00024	-0.13879	-0.04595	0.000094	-0.02147	-0.00433	0.000037	-0.03731	0.001456	-3.9E-05	0.04509	0.001539
1	-0.00019	-0.13505	-0.03336	0.000063	-0.03058	-0.00623	0.000025	-0.03435	-0.00116	-5.9E-05	0.04278	0.004279
1.5	-3.7E-05	-0.09441	-0.02894	0.000014	-0.04289	-0.01139	0.000006	-0.03824	-0.00138	-5E-06	0.040246	0.002419
2	-1.7E-05	-0.04898	-0.02841	0.000019	-0.0478	-0.01138	0.000002	-0.045	-0.00174	0.000018	0.02393	0.000539
3	-6E-06	-0.01073	-0.02185	0.000007	-0.05692	-0.01386	0.000004	-0.04595	-0.00275	0.000016	0.005955	-0.00339
4	0.000006	0.004393	-0.01578	0.000015	-0.06165	-0.01373	-1E-06	-0.04336	-0.00408	0.000025	0.014592	0.001517

Table 2. DSF regression coefficients for vertical spectral ordinates

T(s)	b_{11}	b_{12}	b_{13}	b_{21}	b_{22}	b_{23}	b_{31}	$b_{3,2}$	$b_{3,3}$	$b_{4,1}$	$b_{4,2}$	$b_{4,3}$
0.01	-0.00029	-0.00342	-0.00187	0.000119	0.000371	0.000381	0.000026	0.000491	-0.00012	-8.8E-05	0.001773	-0.00068
0.02	-0.00031	-0.05597	0.001675	0.000125	0.000652	-0.00095	0.000031	0.010212	-8.5E-05	-9.1E-05	-0.0026	0.000641
0.03	-0.00028	-0.21415	0.009371	0.000116	0.003425	0.00118	0.000028	0.040039	-0.00134	-8.7E-05	-0.0177	0.002492
0.04	-0.00025	-0.364	-0.00135	0.000108	0.010125	0.000867	0.000025	0.064891	0.001578	-8.7E-05	-0.02377	0.000605
0.05	-0.00033	-0.44932	-0.01246	0.000106	0.006414	0.00046	0.000046	0.075584	0.00617	-8.2E-05	-0.02308	0.007647
0.075	-0.00027	-0.50139	-0.05554	0.000089	0.008935	0.008159	0.000038	0.064071	0.014079	-5.4E-05	-0.01394	0.0024
0.1	-0.00023	-0.5191	-0.07259	0.00008	0.005159	0.007606	0.000028	0.056524	0.01438	-6.1E-05	-0.01704	-0.00658
0.15	-0.00026	-0.43855	-0.09261	0.000071	0.005295	0.010237	0.000038	0.023424	0.016633	-4.8E-05	-0.02221	-0.00241
0.2	-0.00029	-0.37687	-0.09381	0.000096	0.011892	0.01294	0.000037	0.005606	0.014086	-6.5E-05	0.003151	-0.00635
0.3	-0.00015	-0.34112	-0.07804	0.000058	-0.00207	0.009455	0.000015	-0.00127	0.00791	-4.7E-05	0.005794	-0.0085
0.4	-0.00022	-0.2894	-0.07233	0.000073	-0.00218	0.007109	0.000032	-0.01565	0.006173	-5.3E-05	0.005169	-0.0109
0.5	-0.00021	-0.26291	-0.06316	0.000074	-0.00911	0.00364	0.000024	-0.01769	0.004119	-6.9E-05	0.026225	-0.0058
0.75	-0.00015	-0.2423	-0.05261	0.000046	-0.01137	-0.00118	0.000022	-0.01838	0.002491	-2.2E-05	0.035993	0.000521
1	-0.00016	-0.18527	-0.04198	0.000055	-0.0268	-0.00457	0.000018	-0.03339	0.000468	-0.00005	0.006835	0.005904
1.5	0.000001	-0.16354	-0.04588	-3E-06	-0.03119	-0.01098	-2E-06	-0.02959	0.001895	-8E-06	0.018858	0.005967
2	-1.1E-05	-0.12398	-0.03933	-8E-06	-0.04923	-0.00873	0	-0.03158	0.000506	-2.6E-05	0.022217	0.00257
3	0.000046	-0.09286	-0.04558	-2E-06	-0.05368	-0.01234	-9E-06	-0.03143	0.002455	0.000003	-0.00467	-0.00138
4	0.000021	-0.05867	-0.04345	0.000012	-0.05926	-0.0154	-8E-06	-0.03179	0.001561	0	-0.00943	-0.00789

Figure 3 shows the magnitude, distance and V_{S30} scaling of the DSF model for horizontal (left column) and vertical (right column) spectral ordinates at T=0.1s. The effect of damping is prominent at short spectral periods, which is the main reason behind the choice of T = 0.1s. The selected earthquake scenarios are random. The effect of magnitude scaling on DSF is presented on the first raw for a stiff site (V_{S30} = 525 m/s) located R_{JB} = 15km from the causative fault. The influence of magnitude increases with decreasing event size for horizontal ground motions. The vertical spectral ordinates are less sensitive to the variations in magnitude. Distance-dependent scaling of DSF is plotted in the second row on Figure 3 for M_w 6 and V_{S30} = 525 m/s. The effect of distance on damping seems to be more apparent with respect to magnitude. The decay in geometrical spreading of DSF is faster at very low ($\beta<3\%$) and high ($\beta>15\%$) damping ratios. The V_{S30} scaling of DSF that is plotted for M_w 6; R_{JB}=15 km is given in the last of Figure 3. The site class affects the variation of DSF model for horizontal spectral ordinates. The damping scaling of horizontal ground motions grows with increasing V_{S30} up to 1000 m/s and becomes stable after V_{S30} = 1000 m/s. This trend is more visible at lower and higher damping ratios. The damping scaling of vertical spectrum is not very sensitive to the changes in V_{S30}.

Figure 4 compares the horizontal (top row) and vertical (bottom row) DSF models with those of Rezaeian et al. (2012) and Eurocode 8 (CEN, 2004). The Eurocode 8 (CEN, 2004) damping scaling does not depend on period whereas the other two models consider the influence of period on damping scaling. The comparisons are made for two different magnitudes: M_w 4.5 (left column) and M_w 7.5 (right column). The fictitious site is assumed to be on the footwall and its soil condition is defined as rock with V_{S30}=800 m/s. The site is located at a distance of R_{JB} = 10 km from the causative fault. The corresponding rupture distance (R_{rup}) is computed as 11.2 km by assuming that the top of the ruptured fault segment is 5 km below the surface. The comparative plots advocate a fairly good similarity between three DSF models. The proposed DSF model and Rezaeian et al. (2012) differ from each other at very low ($\beta < 3\%$) and high ($\beta > 10\%$) damping levels. The Eurocode 8 (CEN, 2004) damping scaling would result in significantly different spectral ordinates at very short periods with respect to the spectral ordinates modified by the DSF models of this study and

Rezaeian et al. (2012). These differences would be minimum at the mid-period range as damping scaling becomes flat and independent of spectral period.

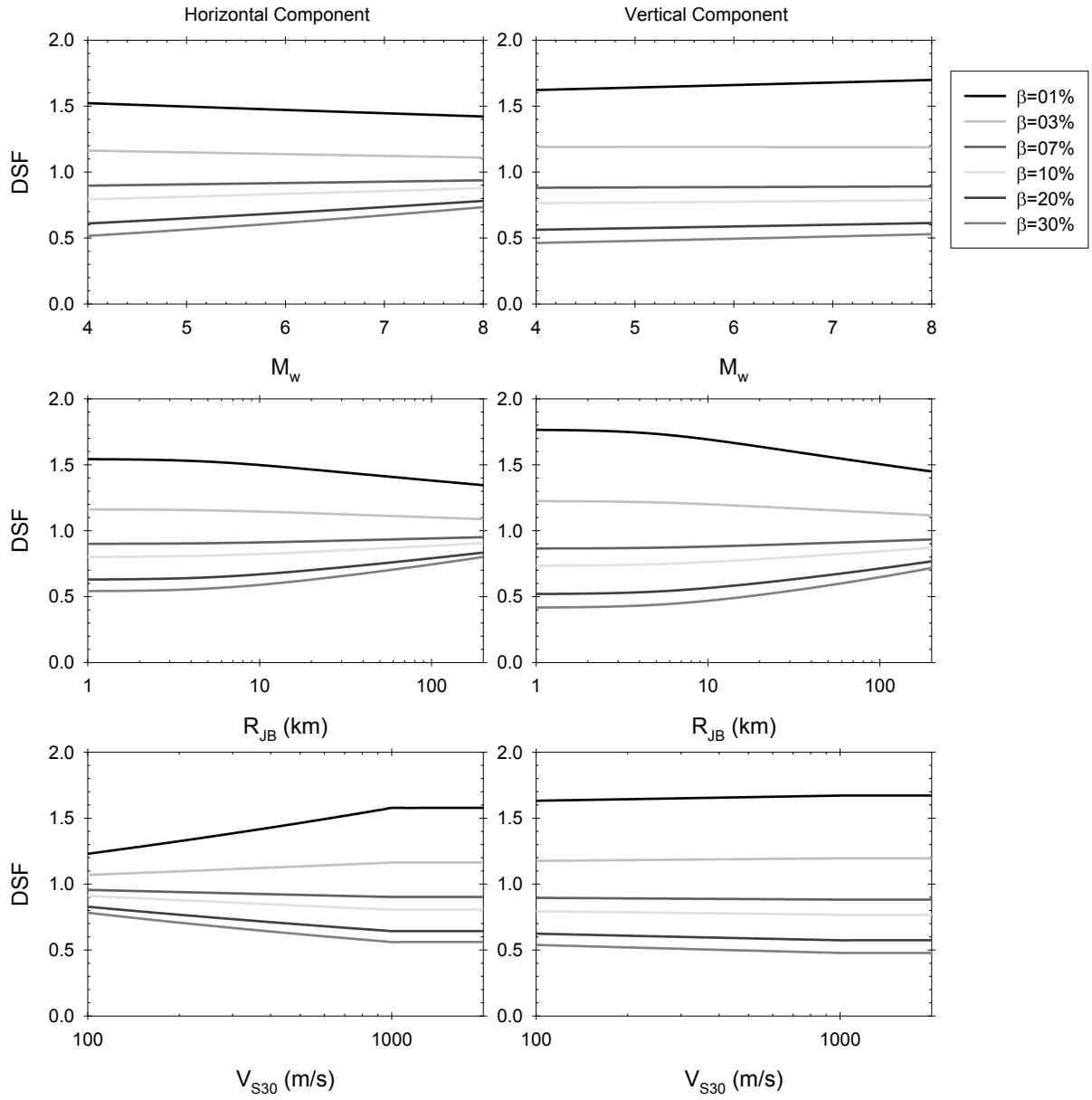

Figure 3. Magnitude (top row), distance (middle row) and V_{S30} (bottom row) scaling for horizontal (left panel) and vertical (right panel) spectra at T=0.1s

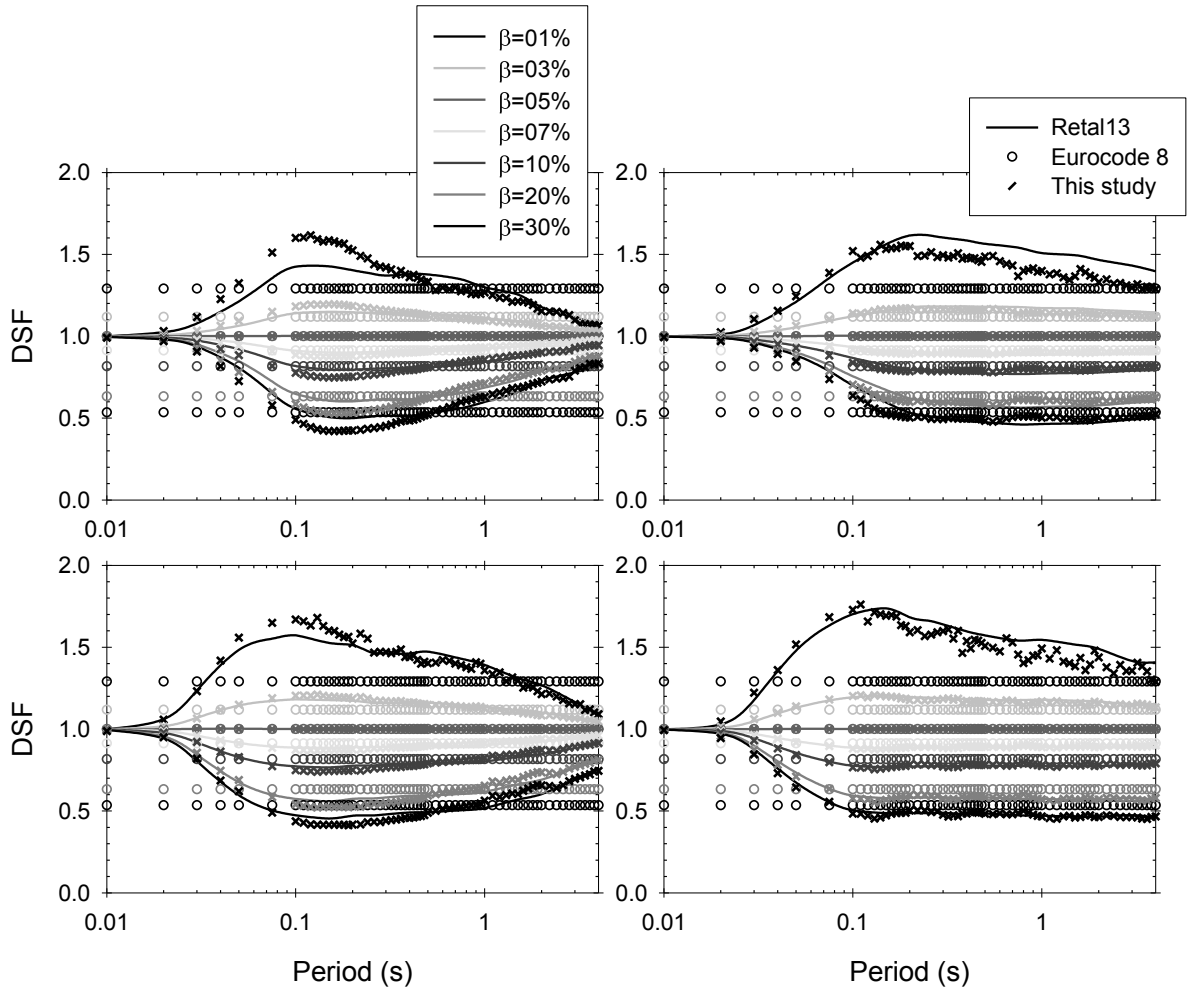

Figure 4. Horizontal (top row) and vertical (bottom row) DSF values of the proposed model as well as Razeian et al (2012) and Eurocode 8 (CEN, 2004) for M_w 4.5 (left panel) and M_w 7.5 (right panel) at R_{JB}=10 km for a rock site of V_{S30}=800 m/s

Vertical-to-Horizontal (V/H) Spectral Amplitude Predictive Model

The vertical probabilistic hazard assessment is important for structures, such as lifeline systems or special components of nuclear power plants, that are prone to seismic risk upon the exceedance of a certain level of vertical displacement (Campbell and Bozorgnia, 2003; Gülerce and Abrahamson, 2011; Bommer et al., 2011). The vertical spectrum also constitutes an important component of structural design for very stiff buildings that can be excited by higher modes due to the particular frequency characteristics of the ground motion (Elnashai and Papazoglu, 1997). The vertical spectrum should be compatible with the horizontal spectrum for a consistent seismic design that can be achieved through vertical-to-horizontal spectral

ratio models. Bozorgnia and Campbell (2004) and Bommer et al. (2011) give a detailed literature survey on the development of vertical ground-motion models.

The proposed vertical-to-horizontal spectral ratio model that can be used in the hazard assessment studies of broader Europe region differs from the recently proposed model of Tezcan and Piolatto (2012) as the later uses non-parametric (data driven) regression technique. Such models cannot be used for earthquake scenarios outside of their applicability range. The proposed model is capable of estimating vertical ground motions for all site conditions that makes it different than the recent vertical ground-motion equations given by Edwards et al. (2011) that is only valid for rock sites. The V/H model of this study shows similarities to the one proposed by Bommer et al. (2011) in terms of regression technique that superseded the previous pan-European GMPE of Ambraseys and Simpson (1996). However, the functional form of the proposed model is more complicated than the Bommer et al. (2011) GMPE and the site effects account for nonlinear soil behaviour, which is disregarded by Bommer et al. (2011). Besides the proposed V/H model is fully compatible with the most recent horizontal pan-European GMPE described in Akkar et al. (2013) because the database, thus all metadata and record processing, is common for both models. This property makes the model even more useful for probabilistic seismic hazard studies that aim at computing horizontal and vertical spectral ordinates at the same time. The specific features of the proposed V/H GMPE are described in the following paragraphs.

The proposed V/H model (Equations 4) uses a functional form similar to that of Gülerce and Abrahamson (2011) study but employs data only from the pan-European region. The magnitude scaling consists of a quadratic magnitude term as well as a hinging magnitude (c_1) to account for magnitude saturation effects. The model considers magnitude dependency in geometrical spreading and describes the soil effects with a nonlinear site function that is based on V_{S30} and PGA at the reference rock site. The effect of faulting mechanism on V/H is addressed by dummy variables F_N and F_R that are unity for normal and reverse faults, respectively, and zero otherwise. These terms also exist in the Akkar et al. (2013) horizontal pan-European ground-motion model that result in a compatible set of predictive equations for describing the horizontal and vertical spectral demand on structural systems.

$$\ln(V/H)=\begin{cases} a_1+a_2(M_w-c_1)+a_3(8.5-M_w)^2+\left[a_4+a_5(M_W-c_1)\right]\ln(\sqrt{R_{JB}^2+a_6{}^2})+ \\ a_8F_N+a_9F_R+S \qquad \text{for } M_w\le c_1 \\ a_1+a_7(M_w-c_1)+a_3(8.5-M_w)^2+\left[a_4+a_5(M_W-c_1)\right]\ln(\sqrt{R_{JB}^2+a_6{}^2})+ \\ a_8F_N+a_9F_R+S \qquad \text{for } M_w>c_1 \end{cases} \tag{4.a}$$

$$S=\begin{cases} a_{10}\ln(V_{S30}/V_{REF})-a_{11}\ln\left[\dfrac{PGA_{REF}+c(V_{S30}/V_{REF})^n}{(PGA_{REF}+c)(V_{S30}/V_{REF})^n}\right] & \text{for } V_{S30}\le V_{REF} \\ a_{10}\ln\left[\dfrac{\min(V_{S30},1000)}{V_{REF}}\right] & \text{for } V_{S30}>V_{REF} \end{cases} \tag{4.b}$$

$$\ln(PGA_{REF})=\begin{cases} \text{for } M_w\le c_1 \quad 1.85329+0.0029(M_w-c_1)-0.02807(8.5-M_w)^2+ \\ \left[-1.23452+0.2529(M_W-c_1)\right]\ln(\sqrt{R_{JB}^2+7.5^2})-0.1091F_N+0.0937F_R \\ \text{for } M_w>c_1 \quad 1.85329-0.5096(M_w-c_1)-0.02807(8.5-M_w)^2+ \\ \left[-1.23452+0.2529(M_W-c_1)\right]\ln(\sqrt{R_{JB}^2+7.5^2})-0.1091F_N+0.0937F_R \end{cases} \tag{4.c}$$

The regression coefficients a_1 to a_{10} are computed from mixed-effects regression algorithm of Abrahamson and Youngs (1992). The magnitude and source-to-site distance measures are moment magnitude (M_w) and Joyner-Boore distance (R_{JB}) that are now almost standard in most of the predictive models in Europe. The hinging magnitude 'c_1' is taken as 6.75 in order to provide compatibility with the horizontal GMPE of Akkar et al. (2013). The fictitious depth and the coefficients of linear magnitude terms (a_2 and a_7) are held fixed for the entire period range for a smooth spectral shape. The site amplification function, designated by S in Eq. 4.b, includes both linear and nonlinear soil amplification. The nonlinearity is considered by the reference peak ground acceleration (PGA_{REF}) that is computed for V_{S30}=750 m/s (see Eq. 4.c). The V_{S30} value of 750 m/s defines reference rock conditions in the V/H nonlinear site model, which is also the case in the nonlinear site function of Akkar et al. (2013) horizontal GMPE. The nonlinearity related coefficients 'c', 'n', and a_{11} are adopted from the Sandıkkaya et al. (2013) site model.

The nonlinear site behavior in the V/H model deserves some more discussion. The soil amplification of V/H inherently depends on the site behavior of vertical and horizontal acceleration components and it has yet to be better understood. In horizontal ground motions, the amplification trend is predominantly nonlinear at high ground-motion intensity levels for low V_{S30} sites (Chio and Steward, 2005; Walling et

al. 2008; Sandıkkaya et al. 2013). There is no clear evidence on the nonlinear site behavior of vertical ground motions (Campbell and Bozorgnia, 2003; Kalkan and Gülkan, 2004; Ambraseys et al., 2005; Cauzzi and Facciolli, 2008; Gülerce and Abrahamson, 2011; Bommer et al., 2011). Thus, implementation of soil nonlinearity in the V/H GMPE is rather conceptual as in the case of Gülerce and Abrahamson (2011) and it is achieved by means of subtracting the horizontal soil nonlinearity from the site model. Although this procedure is followed while establishing the nonlinear site function of the proposed model, the final decision on the adaptation of nonlinear soil behavior in the final model is given by comparing the V/H estimations and the residual trends of alternative equations that either consider or disregard the nonlinear site effects. The details of decision process are discussed in the following paragraphs.

Alternative V/H models with and without nonlinear site behavior are compared in Figures 5 and 6 in terms of magnitude scaling. The linear site behavior is simulated by setting a_{11} to zero in Eq. (4.b). This regression coefficient is constrained to the value given in the Sandıkkaya et al. (2013) nonlinear site model to simulate the nonlinear soil behavior. Each plot on these figures is generated for a strike-slip earthquake. The site is assumed to be a soft site and it is represented by V_{S30} = 250m/s in Figure 5 whereas the site condition is considered as rock with V_{S30} = 750m/s in Figure 6. The source-to-site distances are selected as R_{JB} = 5 km and R_{JB} = 150 km in the left and right columns, respectively on both figures. The top, middle and bottom rows on each figure show the estimations for PGA (T = 0s), and spectral ordinates at T = 0.2s and T = 1.0s, respectively.

Figure 5 depicts that both linear and nonlinear models yield similar median V/H estimations at long distances (represented by R_{JB} =150 km) for the entire magnitude range. As distance decreases (represented by R_{JB} = 5 km) the difference in the median V/H estimations of linear and nonlinear models becomes prominent in short-period spectral ordinates (i.e., T = 0s and T = 0.2s) towards larger magnitudes. The nonlinear V/H model yields larger median V/H median estimations than the linear model for these cases emphasizing the effect of nonlinear soil behavior on short-period horizontal spectral ordinates: smaller spectral amplitudes at softer sites for large magnitude events that result in larger V/H estimations. This observation also suggests that the influence of nonlinear soil behavior is limited on short-period

vertical spectral ordinates even for large magnitude and short distances. Figure 6 that shows similar comparative plots for a rock site of V_{S30} = 750 m/s indicates that linear and nonlinear site models of this study yield similar median V/H estimations at short distances (R_{JB} = 5 km) regardless of magnitude range. This behavior is expected as soil nonlinearity would be negligible for rock sites and it has been proven by many studies in the literature (see Sandıkkaya et al., 2013 for detailed discussions on this topic). The same figure points consistently larger V/H estimations of nonlinear model with respect to the linear model for the long-distance case (i.e., R_{JB} = 150 km). This phenomenon may be interpreted as relatively lower rock spectral amplifications of horizontal ground motions with respect to those of vertical ground motions which seem to be independent of spectral period. This observation is controversial to the previous research on soil-dependent spectral amplification because none of such studies showed evidence on the prominence of soil nonlinearity for rock sites at long distances from the seismic source.

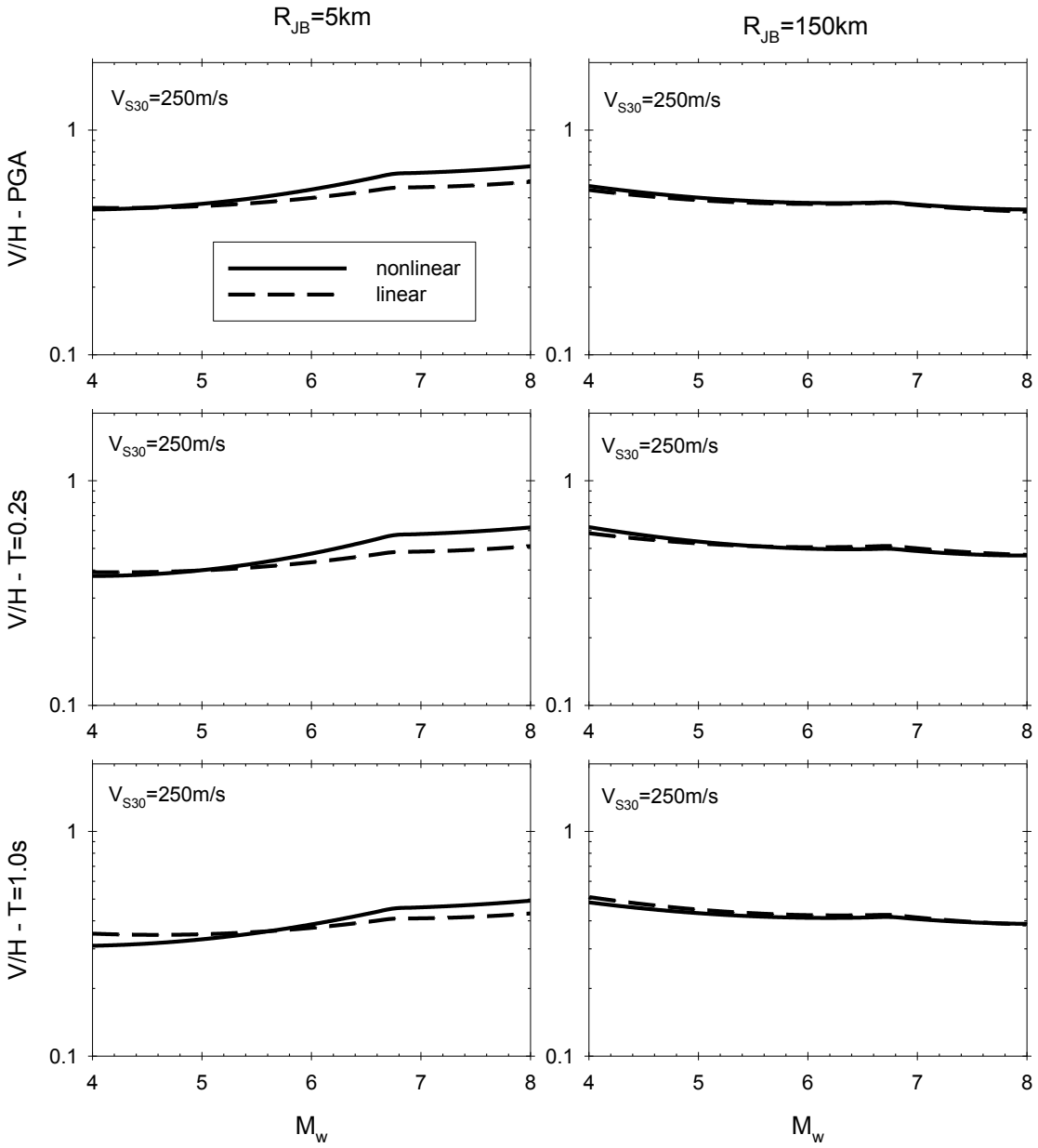

Figure 5. Magnitude scaling of V/H model with and without nonlinear site term for a soft site represented by V_{S30} = 250 m/s

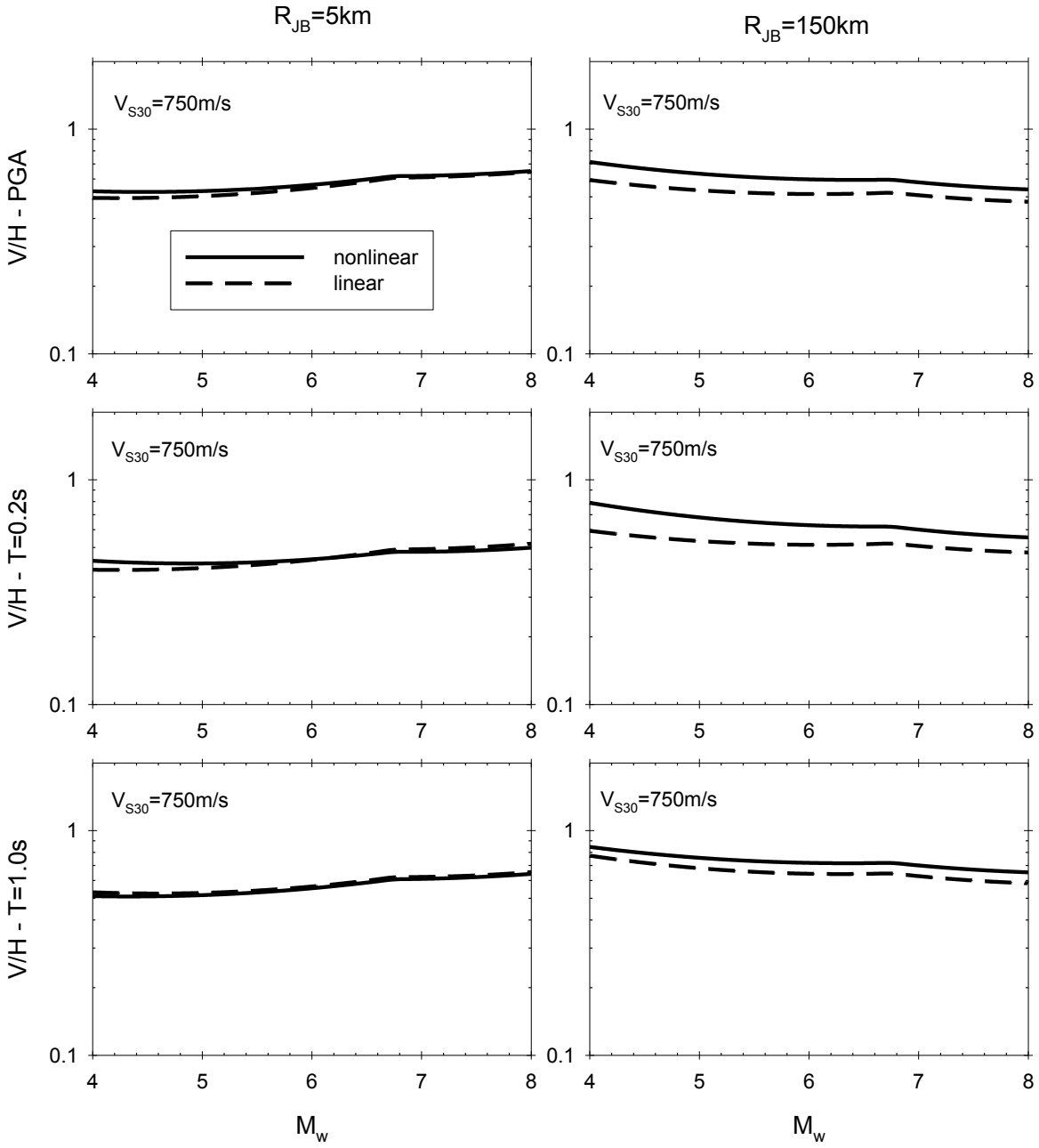

Figure 6. Magnitude scaling of V/H model with and without nonlinear site term for a soft site represented by V_{S30} = 750 m/s

The above discussions on alternative V/H models reveal some unexpected trends when soil nonlinearity is included in the site function. Figure 7 shows the within-event residual scatters in terms of V_{S30} for linear (left panel) and nonlinear (right panel) V/H models. The scatters are plotted for T = 0.2s. The residual scatters are divided into different V_{S30} intervals (designated by vertical dashed lines on Figure 7) and the average residual trend is computed for each V_{S30} interval to better assess the performance of V/H model with and without nonlinear site term. The residuals of

alternative V/H models suggest slightly biased V/H estimations for rock sites (i.e., V_{S30} > 750 m/s) although the level of bias is lesser for the model that disregards soil nonlinearity (left panel on Figure 7). The V/H model with nonlinear site term yields unbiased estimations for very soft sites (i.e., V_{S30} ≤ 180 m/s) with respect to its alternative. Although not given here due to space limitations, the better residual distribution of the nonlinear V/H model for soft soil conditions is observed for 0.2s ≤ T ≤ 0.75s. The unbiased soft-site estimations are the major driving factor for adapting the nonlinear site function in the final V/H model whose regression coefficients are listed in Table 3.

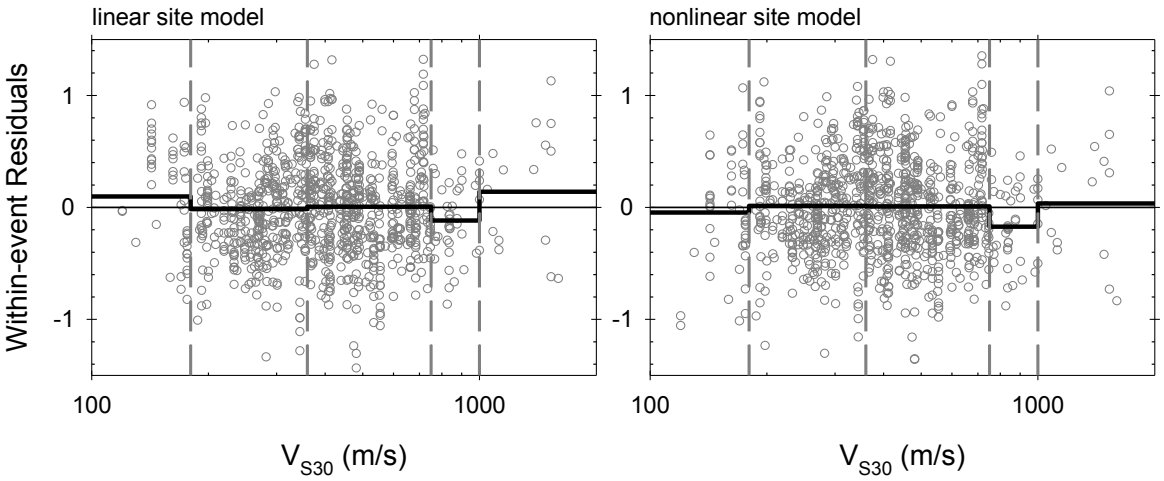

Figure 7. Intra-event residual distributions for the V/H model with and without soil nonlinearity at T=0.2s

Table 3. Period-dependent regression coefficients of the V/H ground-motion model. Period-independent coefficients are given in the footnote

Period (s)	a_1	a_3	a_4	a_8	a_9	a_{10}	a_{11}	σ_w	σ_b	σ_t
PGA	-0.62153	0.033	-0.00551	0.038	0	0.21305	-0.28846	0.3591	0.0635	0.3647
PGV	-0.90001	0.028	0.06617	0.105	0.104	0.36272	-0.19688	0.3648	0.0408	0.3671
0.01	-0.61063	0.033	-0.0075	0.04	0	0.20738	-0.28685	0.3583	0.0722	0.3655
0.02	-0.5319	0.033	-0.02241	0.041	0	0.21266	-0.28241	0.3565	0.0846	0.3664
0.03	-0.32761	0.033	-0.06479	0.036	-0.016	0.20443	-0.26842	0.3625	0.0951	0.3748
0.04	-0.16572	0.031	-0.09718	0.019	-0.046	0.17223	-0.24759	0.3736	0.1236	0.3935
0.05	-0.14158	0.025	-0.10507	0.002	-0.072	0.11084	-0.22385	0.3934	0.1391	0.4173
0.075	-0.29513	0.022	-0.05828	0.003	-0.096	0.06745	-0.17525	0.4059	0.1556	0.4347
0.1	-0.51697	0.018	-0.00766	0.008	-0.1	0.09692	-0.29293	0.4114	0.1924	0.4542
0.2	-1.04455	0.033	0.09008	0.047	-0.006	0.21356	-0.44644	0.44	0.092	0.4495
0.3	-1.03658	0.037	0.08186	0.07	0.038	0.31389	-0.4573	0.4455	0.0249	0.4462
0.4	-0.96249	0.038	0.06927	0.077	0.056	0.38417	-0.43008	0.4493	0.0664	0.4542
0.5	-0.9723	0.038	0.08102	0.081	0.066	0.39799	-0.37408	0.4552	0.0805	0.4623
0.75	-0.74414	0.037	0.04202	0.087	0.076	0.44634	-0.28957	0.4576	0.0256	0.4583
1	-0.73327	0.036	0.05738	0.091	0.083	0.50924	-0.28702	0.4508	0.0252	0.4515
2	-0.58608	0.033	0.02155	0.096	0.092	0.43024	-0.17336	0.4637	0.0449	0.4659
3	-0.47135	0.026	0.01356	0.098	0.097	0.51585	-0.13336	0.4339	0.0767	0.4406
4	-0.45341	0.016	0.00807	0.1	0.1	0.56701	-0.07749	0.4411	0.1208	0.4573

* a_2=0.36; a_5=-0.04; a_6=5; a_7=0.2; c_1=6.75; V_{REF}=750m/s, c=2.5g; n=3.2

The final V/H model is compared with the Bommer et al. (2011) and Gülerce and Abrahamson (2011) GMPEs. The Bommer et al. (2011) model (BAK11) is the most recent pan-European GMPE and it disregards soil nonlinearity in V/H estimations. The Gülerce and Abrahamson (2011) GMPE (GA11) is derived from the NGA-West1 database (Power et al., 2008) and it accounts for the nonlinear soil behavior on V/H. Figure 8 compares the median V/H estimations of the three models for a small-magnitude (M_w 4.5) and a large-magnitude (M_w 7.5) perfect strike-slip earthquake (i.e., dip angle is 90°). The site conditions are chosen as rock (V_{S30} = 750 m/s) and soft (V_{S30} = 250 m/s). The distance range in the comparisons is up to R_{JB} = 200 km. The first 2 panel comparisons show the distance-dependent variation of these models for rock conditions and for PGA (1st row) and T = 1.0s (2nd row). The last 2 panels make a similar comparison for the soft site case (3rd and 4th rows constitute PGA and T = 0.2s comparisons, respectively). The first column plots show the small-magnitude (M_w 4.5) behavior of the models whereas the second column plots focus on the large-magnitude (M_w 7.5) trends in the median V/H estimations.

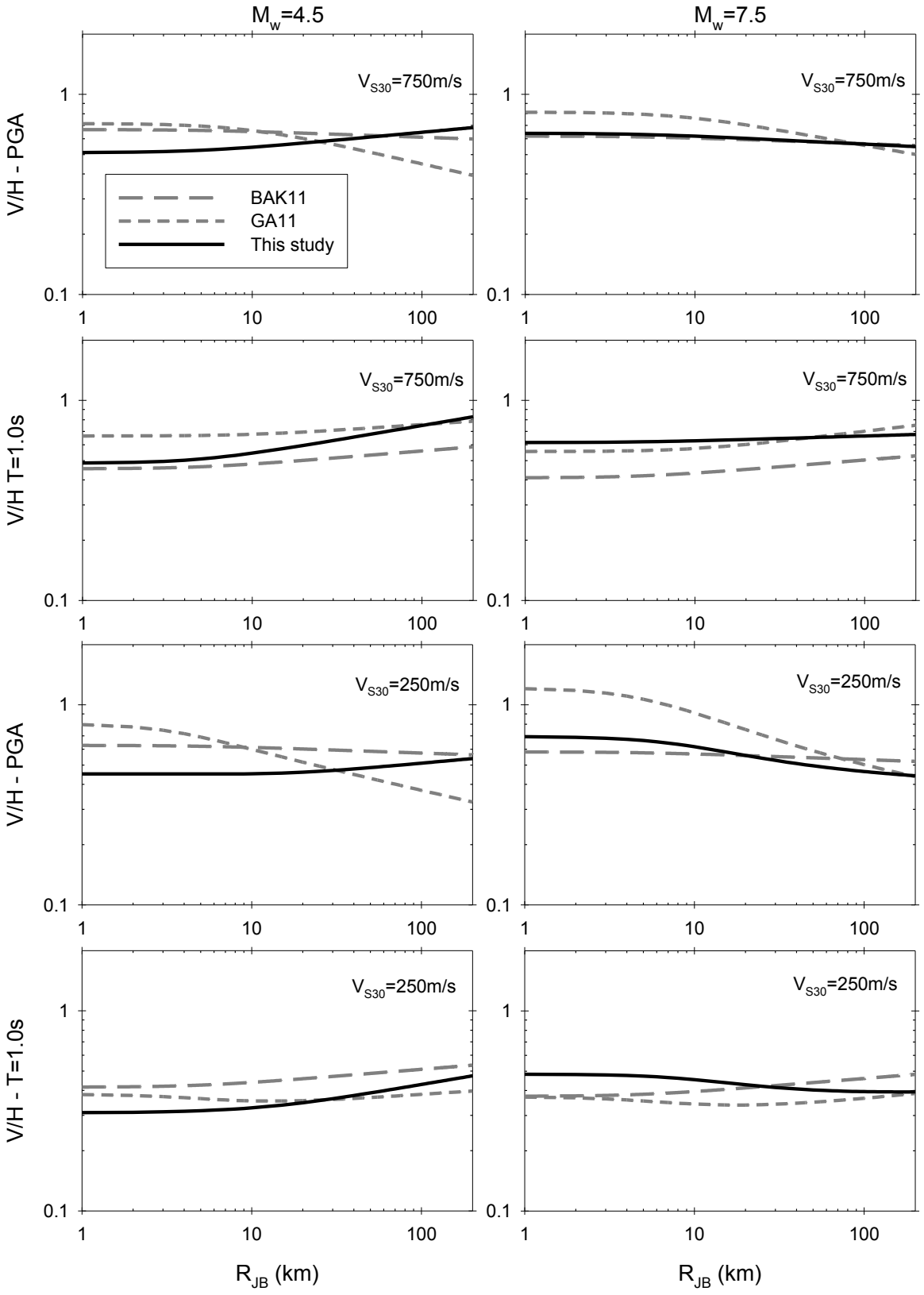

Figure 8. Median V/H estimations of this study as well as those from Bommer et al. (2011) and Gülerce and Abrahamson (2011) GMPEs for different earthquake scenarios.

The median V/H estimations of the proposed model depict differences with respect to BAK11 and GA11. Although this study makes use of the base functional form of GA11 that considers soil nonlinearity in V/H estimations, the discrepancy between the median V/H curves of GA11 and the proposed model is significant in almost all cases. The observed differences between the median V/H estimations of this study and GA11 are more prominent at short spectral periods (represented by T = 0s in Figure 8). The overall short-period median V/H curves of GA11 tend to estimate decreasing V/H with increasing distance, which is exactly the opposite trend in the proposed model. The lower short-period V/H estimations of GA11 towards large distances may indicate the faster distance decay of high-frequency vertical spectral ordinates with respect to the corresponding horizontal spectral ordinates. The database used by Gülerce and Abrahamson (2011) consists of strong-motion recordings from the Western United States (WUS) and Taiwan and the aforementioned feature in GA11 can be a region-specific property of their database. The median V/H estimations of GA11 are larger than those of this study for high-frequency spectral ordinates at short distances which can be the attribute of higher soil nonlinearity in GA11. The differences between GA11 and the proposed model are lesser with increasing spectral period where soil nonlinearity starts losing its significance. The discrepancy between the median V/H estimations of BAK11 and the proposed model are still visible in almost all cases but they are not as significant as those discussed for GA11. This study uses a more complicated functional form that considers magnitude-dependent geometrical spreading as well as linear and nonlinear soil behavior as a function of continuous V_{S30}. These features are not included in BAK11 that may be a reason for the observed differences. Both models are developed from pan-European databases that can partially explain the lesser discrepancy in their median V/H estimations.

Figure 9 compares the median V/H estimations of the above three models for the entire period range considered by the proposed model. The comparisons are done for median V/H trends as this spectral quantity is used in constructing the vertical spectrum compatible to the horizontal spectral ordinates for scenario-specific probabilistic hazard assessment. The details of this methodology are described in the subsequent section. The spectral comparisons in Figure 9 are done for R_{JB} = 10 km for M_w 5, 6 and 7 (left, middle and right columns, respectively). Each row

compares the median V/H estimations for different soil conditions that are consistent with the Eurocode 8 (CEN, 2004) site classification. The first and last rows represent the A/B (V_{S30}=800m/s) and C/D (V_{S30}=180m/s), site class boundaries in Eurocode 8, respectively. The second and third rows characterize site class B (V_{S30}=525m/s) and site class C (V_{S30}=255m/s) soil conditions. The overall observations from Figure 9 justify the discussions made over the comparative plots of Figure 8. The short-period V/H estimations of GA11 are larger than the other two GMPEs and the differences increase as VS30 attains lower values. The difference in the V/H estimations of three GMPEs decreases towards longer periods regardless of the variations in magnitude and site class as the influence of nonlinear soil behavior diminishes in the long-period range. The median V/H estimations of this study follow a very similar trend to that of BAK11.

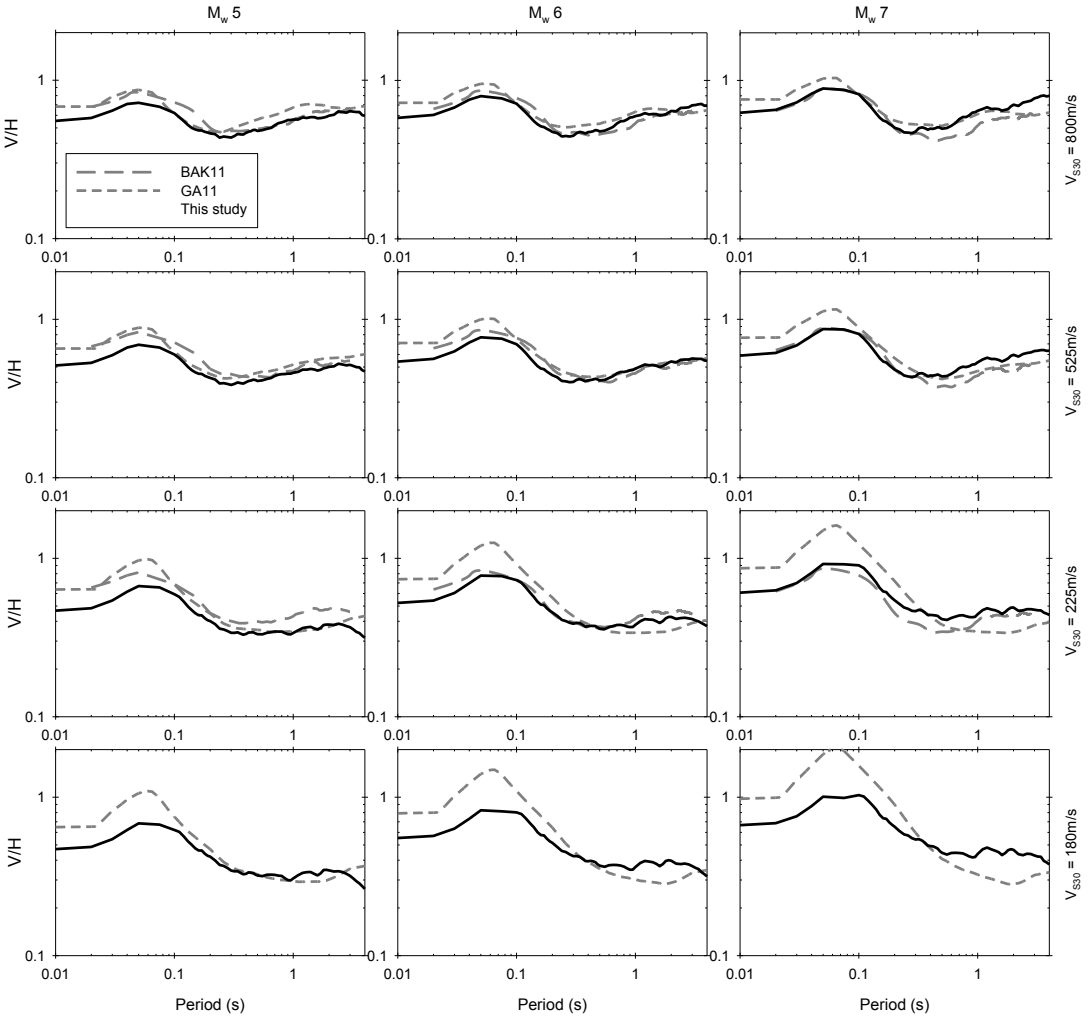

Figure 9. Comparison of the proposed equation with Gülerce and Abrahamson (2011; GA11) and Bommer et al. (2011; BAK11) equations for different magnitudes and site conditions at R_{JB}=30km

5. Developing Consistent Horizontal and Vertical Spectra from Scenario-Specific Probabilistic Seismic Hazard Assessment

Gulerce and Abrahamson (2011) discussed the importance of conditional mean spectrum (CMS) concept (Baker, 2011) and V/H ground-motion models for deriving consistent scenario-based horizontal and vertical design spectra. The proper use of these spectral quantities result in spectral ordinates controlled by the same critical earthquake scenario obtained from the deaggregation of a PSHA study. The resulting horizontal and vertical spectral shapes will also be more realistic as the CMS concept considers the actual correlation of the variability of the ground motion at different spectral periods. The consistent horizontal and vertical spectra essentially will lead to rational selection and scaling of horizontal and vertical ground motions for a specific target earthquake scenario.

The proposed V/H model is entirely compatible with the Akkar et al. (2013) GMPE derived for horizontal spectral ordinates as both studies used exactly the same ground-motion database. This particular property is used to derive the necessary components for calculating compatible horizontal and vertical spectra for scenario-based probabilistic seismic hazard studies. The most recent pan-European V/H model GMPE proposed by Bommer et al. (2011) did not derive these components for the computation of consistent horizontal and vertical spectra from their model as the dataset used in that paper was not employed by any other study for deriving pan-European GMPEs for horizontal spectral ordinates.

The most complete form of consistent horizontal and vertical spectra through the conditional mean spectrum concept and V/H ground-motion model is given in Eqs. (5). The details of this topic can be found in Gulerce and Abrahamson (2011).

$$CMS_{HOR}(T,T_0) = \mu_{HOR}(T) \cdot \exp\left(\rho_{H,t}(T,T_0)\varepsilon(T_0)\sigma_{H,t}(T)\right) \tag{5.a}$$

$$\sigma(T,T_0) = \sigma_{H,t}(T_i) * \sqrt{\left(1-\rho^2_{H,t}(T,T_0)\right)} \tag{5.b}$$

$$CMS_{VER}(T,T_0) = CMS_{HOR}(T,T_0) * \frac{V}{H}(T,T_0) * \exp(\rho_{H,V/H}(T,T_0) * \sigma_{V/H}) \tag{5.c}$$

$$\rho_{H,V/H}(T_i,T_j) = \frac{\sigma_H(T_i)\sigma_{V/H}(T_j)\rho_w(T_i,T_j) + \tau_H(T_i)\tau_{V/H}(T_j)\rho_b(T_i,T_j)}{\sigma_{H,t}(T_i)\sigma_{V/H,t}(T_j)} \tag{5.d}$$

In the above expressions $\mu_{HOR}(T)$ is the median estimations of the horizontal GMPE for the most contributing earthquake scenario identified after deaggregation analysis for the reference period T_0. The parameter $\sigma_{H,t}(T)$ is the total standard deviation of the horizontal ground-motion model and $\varepsilon(T_0)$ represents the epsilon (number of total standard deviations of horizontal GMPE between median estimation and the most contributing earthquake scenario spectral ordinate at T_0) at the reference spectral period T_0. The correlation coefficient between $\varepsilon(T_0)$ and the period T is defined by $\rho_{H,t}(T,T_0)$. Eq. (5.b) defines the variability associated with the horizontal-component CMS (i.e., $CMS_{HOR}(T,T_0)$) derived by considering the target hazard demand at the reference period T_0 (Lin et al., 2012). The vertical CMS ($CMS_{VER}(T,T_0)$) that is consistent with $CMS_{HOR}(T,T_0)$ for the most contributing earthquake scenario is given in Eq. (5.c). The median V/H estimations computed for the most contributing earthquake scenario ($V/H(T,T_0)$) is multiplied by $CMS_{HOR}(T,T_0)$. The total correlation between the horizontal GMPE and V/H ground-motion model that accounts for the ground motion variability between these two models for periods other that T_0 is given by $\rho_{H,V/H}(T,T_0)$ in Eq. (5.c). The total standard deviation of V/H ground-motion model is $\sigma_{V/H}(T)$. Equation (5.d) is the expression used for computing $\rho_{H,V/H}(T,T_0)$. In this equation σ_H, $\sigma_{V/H}$, $\sigma_{H,t}$, $\sigma_{V/H,t}$, τ_H, $\tau_{V/H}$ are within-event sigma of the horizontal GMPE, within-event sigma of the V/H GMPE, total sigma of the horizontal GMPE, total sigma of the V/H GMPE, between-event sigma of horizontal GMPE and between-event sigma of V/H GMPE, respectively. The within-event and between-event correlation coefficients between the horizontal and V/H GMPEs are represented by ρ_w and ρ_b, respectively. Tables 4, 5 and 6 list the period-dependent correlation coefficients of $\rho_{H,t}(T,T_0)$, ρ_w and ρ_b, respectively. These correlation coefficients are computed from the horizontal GMPE proposed in Akkar et al. (2013) and the V/H model proposed in this study.

Table 4. Period-dependent correlation coefficients of $\rho_{H,t}$

Period (s)	0.01	0.02	0.03	0.04	0.05	0.075	0.1	0.2	0.3	0.4	0.5	0.75	1	2	3	4
0.01	-0.38359	-0.36938	-0.33659	-0.31298	-0.34068	-0.29593	-0.3307	-0.32162	-0.27664	-0.27484	-0.21364	-0.20792	-0.14502	-0.10469	-0.09092	-0.13665
0.02	-0.38219	-0.36976	-0.33631	-0.31378	-0.34209	-0.29952	-0.33262	-0.32357	-0.27598	-0.2692	-0.20924	-0.20863	-0.14661	-0.10684	-0.09334	-0.13733
0.03	-0.37673	-0.36197	-0.32894	-0.30785	-0.34656	-0.30931	-0.34351	-0.32425	-0.26999	-0.25453	-0.19515	-0.19592	-0.13929	-0.10621	-0.09247	-0.13394
0.04	-0.36392	-0.34684	-0.30764	-0.30037	-0.34958	-0.31788	-0.34942	-0.31449	-0.25322	-0.2348	-0.17757	-0.18205	-0.12151	-0.10831	-0.09145	-0.13529
0.05	-0.34456	-0.32589	-0.28184	-0.27266	-0.34303	-0.32442	-0.35542	-0.31802	-0.24758	-0.22063	-0.16227	-0.16856	-0.10682	-0.10197	-0.08206	-0.12164
0.075	-0.3258	-0.30753	-0.26491	-0.23036	-0.27284	-0.3519	-0.37176	-0.33544	-0.2391	-0.21088	-0.13989	-0.15358	-0.09921	-0.06969	-0.05106	-0.09665
0.1	-0.33554	-0.31848	-0.28365	-0.24618	-0.27211	-0.29577	-0.40583	-0.3479	-0.23461	-0.21239	-0.14001	-0.1434	-0.08801	-0.05195	-0.02784	-0.08541
0.2	-0.33346	-0.32686	-0.30319	-0.27466	-0.26814	-0.2029	-0.25662	-0.40178	-0.29953	-0.29164	-0.21735	-0.20334	-0.15744	-0.06811	-0.04185	-0.10026
0.3	-0.27235	-0.27285	-0.275	-0.2507	-0.21225	-0.13138	-0.1528	-0.22419	-0.36775	-0.35042	-0.27344	-0.24146	-0.1781	-0.11267	-0.09458	-0.14659
0.4	-0.24947	-0.25221	-0.26541	-0.23975	-0.19897	-0.09786	-0.10293	-0.15596	-0.2728	-0.40079	-0.30919	-0.27891	-0.20245	-0.13302	-0.13206	-0.15345
0.5	-0.22016	-0.22365	-0.24348	-0.22184	-0.18018	-0.07384	-0.06419	-0.1131	-0.18951	-0.29917	-0.31512	-0.2844	-0.21939	-0.1578	-0.17705	-0.19253
0.75	-0.14444	-0.15128	-0.17649	-0.16963	-0.13617	-0.04401	-0.01026	-0.02226	-0.10524	-0.1638	-0.16034	-0.29202	-0.23279	-0.1906	-0.19977	-0.23702
1	-0.11147	-0.12046	-0.14667	-0.14167	-0.10574	-0.01795	-0.00605	0.014721	-0.07004	-0.10419	-0.08497	-0.18073	-0.24267	-0.21313	-0.22096	-0.2576
2	-0.04541	-0.0496	-0.06769	-0.07777	-0.06379	0.016613	0.018271	0.066084	-0.04465	-0.0677	-0.0377	-0.04063	-0.03389	-0.26276	-0.2812	-0.31153
3	-0.02874	-0.02927	-0.04742	-0.05455	-0.03734	0.043795	0.019973	0.052634	-0.02918	-0.06708	-0.04628	-0.01577	-0.00344	-0.11905	-0.33448	-0.37408
4	-0.01351	-0.01769	-0.03401	-0.04337	0.000794	0.066529	0.040807	0.029078	-0.05561	-0.06745	-0.04074	-0.00077	-0.01269	-0.09263	-0.29442	-0.43695

Table 5. Period-dependent correlation coefficients of ρ_b

Period (s)	0.01	0.02	0.03	0.04	0.05	0.075	0.1	0.2	0.3	0.4	0.5	0.75	1	2	3	4
0.01	-0.40739	-0.3921	-0.35701	-0.33795	-0.37544	-0.3172	-0.35036	-0.33966	-0.29606	-0.29855	-0.23014	-0.22247	-0.14798	-0.11922	-0.10498	-0.15549
0.02	-0.40283	-0.38953	-0.35399	-0.33653	-0.37485	-0.31812	-0.34867	-0.33963	-0.29457	-0.29223	-0.2255	-0.22314	-0.14897	-0.12213	-0.10805	-0.15751
0.03	-0.39362	-0.37777	-0.34323	-0.3274	-0.37681	-0.32576	-0.3558	-0.33608	-0.28517	-0.27502	-0.20914	-0.20725	-0.13928	-0.12053	-0.10688	-0.15468
0.04	-0.37575	-0.35754	-0.31723	-0.31738	-0.37681	-0.33015	-0.35596	-0.31979	-0.26477	-0.25296	-0.18916	-0.1897	-0.11774	-0.11987	-0.10453	-0.15795
0.05	-0.35635	-0.33602	-0.29053	-0.28855	-0.37126	-0.33846	-0.36237	-0.32161	-0.25785	-0.23932	-0.17295	-0.17252	-0.10219	-0.11255	-0.09344	-0.14259
0.075	-0.33797	-0.31796	-0.27301	-0.24541	-0.30204	-0.37315	-0.38067	-0.34035	-0.24664	-0.2299	-0.14742	-0.15448	-0.09351	-0.07766	-0.06235	-0.11537
0.1	-0.34173	-0.32205	-0.28597	-0.25909	-0.30233	-0.30954	-0.41653	-0.35132	-0.23795	-0.23171	-0.1465	-0.14151	-0.07643	-0.05973	-0.04192	-0.10083
0.2	-0.35705	-0.35021	-0.32447	-0.30052	-0.30081	-0.22141	-0.27736	-0.43096	-0.32278	-0.31476	-0.23496	-0.22082	-0.16093	-0.07614	-0.04865	-0.1126
0.3	-0.30622	-0.30704	-0.30973	-0.28459	-0.24381	-0.1493	-0.17376	-0.25319	-0.41589	-0.39438	-0.30768	-0.27255	-0.19778	-0.12829	-0.10787	-0.16599
0.4	-0.27107	-0.27476	-0.29164	-0.26867	-0.2295	-0.1096	-0.11771	-0.16789	-0.30025	-0.43783	-0.33864	-0.3058	-0.21658	-0.14972	-0.1479	-0.17021
0.5	-0.24079	-0.2456	-0.27013	-0.25147	-0.21037	-0.08327	-0.07484	-0.1229	-0.211	-0.32644	-0.34742	-0.31505	-0.23966	-0.17864	-0.1988	-0.21692
0.75	-0.16215	-0.17036	-0.20023	-0.19429	-0.15754	-0.04987	-0.01187	-0.02403	-0.1211	-0.1854	-0.18189	-0.33276	-0.26595	-0.2188	-0.22908	-0.2727
1	-0.12273	-0.13345	-0.16397	-0.15993	-0.12088	-0.01898	-0.00604	0.018085	-0.08088	-0.117	-0.09494	-0.20467	-0.27607	-0.24422	-0.25135	-0.29527
2	-0.04597	-0.05102	-0.07144	-0.08378	-0.06961	0.020182	0.022916	0.074428	-0.05138	-0.07591	-0.04184	-0.04698	-0.0395	-0.29465	-0.31286	-0.34993
3	-0.01897	-0.02017	-0.04131	-0.05323	-0.03739	0.054725	0.031627	0.064147	-0.0391	-0.08116	-0.05672	-0.02728	-0.01099	-0.14482	-0.37809	-0.43317
4	-0.00669	-0.01091	-0.0292	-0.04188	0.005346	0.071296	0.048348	0.033106	-0.07387	-0.08209	-0.05485	-0.01744	-0.0312	-0.1185	-0.33607	-0.49362

Table 6. Period-dependent correlation coefficients of ρ_w

Period (s)	0.01	0.02	0.03	0.04	0.05	0.075	0.1	0.2	0.3	0.4	0.5	0.75	1	2	3	4
0.01	-0.36374	-0.35197	-0.32309	-0.25	-0.20827	-0.25616	-0.32086	-0.32109	-0.24335	-0.20454	-0.17532	-0.18329	-0.18843	-0.03161	-0.01529	-0.04231
0.02	-0.36264	-0.35227	-0.32265	-0.25451	-0.21838	-0.26613	-0.32984	-0.31754	-0.23443	-0.19232	-0.16164	-0.17383	-0.18042	-0.03062	-0.01672	-0.03542
0.03	-0.35363	-0.34265	-0.31186	-0.25047	-0.22673	-0.273	-0.34333	-0.32251	-0.23284	-0.1781	-0.14804	-0.16687	-0.17272	-0.03561	-0.01798	-0.02697
0.04	-0.33898	-0.32651	-0.28898	-0.23611	-0.22997	-0.28438	-0.35445	-0.32261	-0.21585	-0.15527	-0.13032	-0.1591	-0.15964	-0.05244	-0.02427	-0.016
0.05	-0.31525	-0.30406	-0.26339	-0.21138	-0.21797	-0.27971	-0.35543	-0.33329	-0.216	-0.13714	-0.11869	-0.16472	-0.1459	-0.05208	-0.02531	-0.01378
0.075	-0.29914	-0.28777	-0.25253	-0.17806	-0.15191	-0.28109	-0.36708	-0.34746	-0.22672	-0.13585	-0.1165	-0.16606	-0.13986	-0.03613	0.001749	-0.01037
0.1	-0.33196	-0.3243	-0.29227	-0.21015	-0.16858	-0.2594	-0.38871	-0.3562	-0.23606	-0.14866	-0.12292	-0.16	-0.13981	-0.0242	0.026633	-0.0292
0.2	-0.32388	-0.31528	-0.29596	-0.20681	-0.13263	-0.15828	-0.22515	-0.38323	-0.27164	-0.26	-0.1903	-0.16865	-0.22432	-0.03623	-0.0049	-0.04838
0.3	-0.27481	-0.26721	-0.26097	-0.16898	-0.05442	-0.08362	-0.09338	-0.19179	-0.29651	-0.34148	-0.26835	-0.21086	-0.25588	-0.06378	-0.04814	-0.11174
0.4	-0.251	-0.24563	-0.22977	-0.14785	-0.04803	-0.06109	-0.03655	-0.17495	-0.2306	-0.37635	-0.28039	-0.24916	-0.2425	-0.07462	-0.08253	-0.11463
0.5	-0.22753	-0.22019	-0.20961	-0.13252	-0.04057	-0.04883	-0.01553	-0.12565	-0.15496	-0.31744	-0.29532	-0.25014	-0.22992	-0.09677	-0.12651	-0.12946
0.75	-0.19424	-0.18756	-0.17458	-0.11301	-0.04351	-0.04544	-0.00328	-0.05856	-0.05343	-0.17474	-0.15913	-0.24543	-0.17534	-0.11229	-0.12492	-0.12122
1	-0.19649	-0.18705	-0.18214	-0.12823	-0.04919	-0.05548	-0.02962	-0.03184	-0.00752	-0.11335	-0.10708	-0.14356	-0.15419	-0.08123	-0.14106	-0.09555
2	-0.17916	-0.16687	-0.16478	-0.13018	-0.07577	-0.0518	-0.08208	-0.00208	0.039535	-0.00955	-0.02027	0.04399	0.047649	-0.03656	-0.12512	-0.02269
3	-0.16005	-0.15375	-0.15471	-0.11554	-0.06865	-0.03828	-0.09037	-0.02827	0.054382	0.02951	0.028359	0.096579	0.076152	0.060913	-0.14335	-0.0476
4	-0.08595	-0.09236	-0.10035	-0.08453	-0.04139	0.06344	-0.00438	0.009498	0.080831	0.02761	0.066001	0.155044	0.152991	0.091981	-0.08804	-0.17891

Conclusion

This report presents ground-motion models to estimate damping scaling factors and vertical-to-horizontal spectral ratios by using the SHARE ground-motion databank. The proposed models are derived for the vector-based probabilistic hazard assessment studies in the broader pan European region.

References

Abrahamson NA, Silva WJ (1996). *Empirical Ground Motion Models*, Report to Brookhaven National Laboratory.

Abrahamson, N.A. and R.R. Youngs (1992). A stable algorithm for regression analyses using the random effects model, *Bull. Seism. Soc. Am.*, **82**: 505–510.

Akkar S, Bommer JJ (2006) Influence of long-period filter cut-off on elastic spectral displacements. *Earthquake Engineering & Structural Dynamics* **35**:1145-1165.

Akkar S, Bommer JJ (2007) Prediction of elastic displacement response spectra at multiple damping levels in Europe and the Middle East. *Earthquake Engineering & Structural Dynamics* **36:**1275-1301.

Akkar S, Bommer JJ (2010) Empirical equations for the prediction of PGA, PGV and spectral accelerations in Europe, the Mediterranean and the Middle East. *Seismological Research Letters* **81:**195-206.

Akkar S, Çağnan Z, Yenier E, Erdogan Ö, Sandıkkaya MA, Gülkan P, (2010) The recently compiled Turkish strong-motion database: preliminary investigation for seismological parameters, *Journal of Seismology*, **14:** 457-479

Akkar, S., Kale, O., Yenier, E. and Bommer J.J., 2011. The high-frequency limit of usable response spectral ordinates from filtered analogue and digital strong-motion accelerograms, Earthquake Engineering and Structural Dynamics,40,1387-1401.

Akkar S, Sandıkkaya MA, Bommer JJ (2013), Empirical Ground-Motion Models for Point- and Extended-Source Crustal Earthquake Scenarios in Europe and the Middle East, Bulletin of Earthquake Engineering, submitted to this issue.

Akkar S, Sandıkkaya MA, Şenyurt M, Azari AS, Ay BÖ (2013b), Reference database for seismic ground-motion in Europe (RESORCE), Bulletin of Earthquake Engineering, submitted to this issue.

Ambraseys NN, Douglas J, Sarma SK, Smit PM (2005) Equations for the Estimation of Strong Ground Motions from Shallow Crustal Earthquakes Using Data from Europe and the Middle East: Vertical Peak Ground Acceleration and Spectral. *Bulletin of Earthquake Engineering* **3**:54-73.

Ambraseys NN, Smit P, Douglas J, Margaris B, Sigbjörnsson R, Olafsson S, Suhadolc P, and Costa G (2004). Internet site for European strong-motion data, *Bollettino di Geofisica Teorica ed Applicata*, **45:** 113-129.

Ambraseys, N. N., and Douglas, J., 2003. Near field horizontal and vertical earthquake ground motions, Soil Dynamics and Earthquake Engineering 23, 1–18.

Ambraseys, N. N., and K. A. Simpson (1996). The prediction of vertical response spectra in Europe, Earthq. Eng. Struct. Dyn. 25, 401–412.

Ashour SA (1987). Elastic Seismic Response of Buildings with Supplemental Damping, Ph.D. Dissertation, Department of Civil Engineering, University of Michigan, Ann Arbor, MI.

Atkinson GM, Pierre JR (2004). Ground-motion response spectra in eastern North America for different critical damping values, Seismo. Res. Lett., 75:541-545.

Baker, J. W. (2011). Conditional mean spectrum: Tool for ground motion selection. J. Struct.

Baker, J. W. and C. A. Cornell (2006). Spectral shape, epsilon and record selection. Earthq. Eng. Struct. Dynam. 35(9), 1077–1095.

Baker, J.W. and N. Jayaram (2008). Correlation of spectral acceleration values from NGA ground motion models. Earthq. Spectra 24(1), 299–317.

Berge-Thierry C, Cotton C, Scotti O, Griot-Pommera D-A, Fukushima Y (2003) New empirical attenuation laws for moderate European earthquakes. *Journal of Earthquake Engineering* **7**:193-222.

Bommer J, Elnashai AS, Chlimintzas GO, Lee D (1998). Review and development of response spectra for displacement-based design, ESEE Research Report No. 98-3, Imperial College London.

Bommer J, Mendis R (2005). Scaling of spectral displacement ordinates with damping ratios, Earthq. Engrg. Struct. Dyn., 34:145–165.

Bommer JJ, Akkar S, Kale Ö (2011) A model for vertical-to-horizontal response spectral ratios for Europe and the Middle East. Bulletin of the Seismological Society of America 101:1783-1806.

Bommer JJ, Stafford PJ, Alarcón JE, Akkar S (2007) The influence of magnitude range on empirical ground-motion prediction. Bulletin of the Seismological Society of America 97:2152-2170.

Boore DM, Joyner WB, Fumal TE (1993). Estimation of response spectra and peak accelerations from western North American earthquakes: an interim report, US Geological Survey Open-File Report 93-509, Menlo Park, CA.

Bozorgnia, Y., and K. W. Campbell (2004). The vertical-to-horizontal spectral ratio and tentative procedures for developing simplified V/H and vertical design spectra, J. Earthq. Eng. 4, no. 4, 539–561.

BSSC, Building Seismic Safety Council (2009a). 2009 NEHRP Recommended Seismic Provisions For New Buildings and Other Structures: Part 1, Provisions, Federal Emergency Management Agency (P-750), Washington D.C.

Cameron WI, Green I (2007). Damping correction factors for horizontal ground-motion response spectra, Bull. Seismo. Soc. Am., 97:934–960.

Campbell, K. W., and Y. Bozorgnia (2003). Updated near-source ground motion (attenuation) relations for the horizontal and vertical components of peak ground acceleration and acceleration response spectra, Bull. Seismol. Soc. Am. 93, no. 1, 314–331.

Cauzzi, C., and E. Faccioli (2008). Broadband (0.05 to 20 s) prediction of displacement response based on worldwide digital records, J. Seismol. 12, 453–475.

Choi, Y. and J.P. Stewart (2005). Nonlinear site amplification as function of 30m shear wave velocity, Earthquake Spectra, 21: 1-30.

Comité Européen de Normalisation (CEN) (2004). Eurocode 8, Design of structures for earthquake resistance—part 1: General rules, seismic actions and rules for buildings. European Standard NF EN 1998-1, Brussels.

Edwards B, Poggi V, Fäh D (2011) A Predictive Equation for the Vertical-to-Horizontal Ratio of Ground Motion at Rock Sites Based on Shear-Wave Velocity Profiles from Japan and Switzerland. Bulletin of the Seismological Society of America, 101:2998–3019.

Eng. 137(3), 322–331.Berge-Thierry et al., 2003.

Elnashai, A. S., and A. J. Papazoglu (1997). Procedure and spectra for analysis of RC structures subjected to vertical earthquake loads, Journal of Earthquake Engineering, no. 1, 121–155.

Faccioli E, Paolucci R, Rey J (2004). Displacement spectra for long periods, Earthq. Spectra, 20:347–376.

Gülerce, Z., and N. A. Abrahamson (2011). Site-specific spectra for vertical ground motion, Earthq. Spectra, 27: 1023–1047.

Hatzigeorgiou GD (2010). Damping modification factors for SDOF systems subjected to near-fault, far-fault and artificial earthquakes, Earthq. Engrg. Struct. Dyn., 39:1239-1258.

Idriss IM (1993). Procedures for selecting earthquake ground motions at rock sites, Report NIST GCR 93–625, National Institute of Standards and Technology, Washington, D.E.

Lin T, Harmsen SC, Baker JW, Luco N (2012) Conditional Spectrum Computation Incorporating Multiple Causal Earthquakes and Ground Motion Prediction Models, BSSA (in press).

Lin YY, Chang KC (2003). Study on damping reduction factor for buildings under earthquake ground motions, J. Struct. Engrg., 129:206–214.

Lin YY, Chang KC (2004). Effects of site classes on damping reduction factors. J. Struct. Engrg. 130:1667–1675.

Lin YY, Miranda E, Chang KC (2005). Evaluation of damping reduction factors for estimating elastic response of structures with high damping, Earthq. Engrg. Struct. Dyn., 34:1427–1443.

Luzi L, Hailemikael S, Bindi D, Pacor F, Mele F, Sabetta F (2008) ITACA (ITalian ACcelerometric Archive): A web portal for the dissemination of the Italian strong motion data, Seismological Research Letters, 79: 716-722.

Malhotra PK (2006). Smooth spectra of horizontal and vertical ground motions, Bulletin of the Seismological Society of America, 96: 506-518.

Naeim F, Kircher CA (2001). On the damping adjustment factors for earthquake response spectra, The Structural Design of Tall Buildings, 10:361-369.

Newmark NM, Hall WJ (1982). Earthquake Spectra and Design, Earthquake Engineering Research Institute, Berkeley, CA.

Priestley MJN (2003). Myths and Fallacies in Earthquake Engineering, Revisited, The Mallet Milne Lecture, IUSS Press, Istituto Universitario di Studi Superiori di Pavia, Pavia, Italy.

Ramirez OM, Constantinou MC, Kircher CA, Whittaker AS, Johnson MW, Gomez JD, Chrysostomou CZ (2000). Development and evaluation of simplified procedures for analysis and design of buildings with passive energy dissipation systems, Report No: MCEER-00-0010, Multidisciplinary Center for Earthquake Engineering Research, University of New York, Buffalo, NY.

Ramirez OM, Constantinou MC, Whittaker AS, Kircher CA, Chrysostomou CZ (2002). Elastic and inelastic seismic response of buildings with damping systems, Earthq. Spectra, 18:531–547.

Rezaeian S, Bozorgnia Y, Idriss IM, Campbell K, Abrahamson N, Silva W (2012) Spectral Damping Scaling Factors for Shallow Crustal Earthquakes in Active Tectonic Regions. PEER 2012/01, Pacific Earthquake Engineering Research Center, University of California, Berkeley, California.

Sandıkkaya MA, Akkar S, Bard P-Y (2013) A nonlinear site amplification model for the new pan-European ground-motion prediction equations. Bulletin of the Seismological Society of America 103: kk-ll (in press).

Sandıkkaya, M.A., M.T. Yılmaz, B.S. Bakır, and Ö. Yılmaz (2010). Site classification of Turkish national strong-motion stations, Journal of Seismology, 14: 543-563.

Stafford PJ, Mendis R, Bommer, JJ (2008). Dependence of damping correction factors for response spectra on duration and numbers of cycles, ASCE, J Struct. Engrg., 134:1364–1373.

Tezcan J, Piolatto A (2012) A Probabilistic Nonparametric Model for the Vertical-to-Horizontal Spectral Ratio. Journal of Earthquake Engineering, 16: 142-157.

Tolis SV, Faccioli E (1999). Displacement design spectra, J. Earthq. Engrg., 3:107–125.

Trifunac MD, Lee VW (1989). Empirical models for scaling pseudo relative velocity spectra of strong earthquake accelerations in terms of magnitude, distance, site intensity and recording site conditions, Soil Dyn. Earthq. Engrg., 8:126 –144.

Walling, M., W. Silva, and N.A. Abrahamson (2008). Nonlinear Site Amplification Factors for Constraining the NGA Models, Earthquake Spectra, 24: 243-255.

Wu J, Hanson RD (1989). Study of inelastic spectra with high damping, J Struct. Engrg., 115:1412–1431.

Yenier E, Sandikkaya MA and Akkar S (2010) Report on the fundamental features of the extended strong motion databank prepared for the SHARE project, pp. 44.